

Ionic-liquid-gating induced protonation and superconductivity in FeSe, FeSe_{0.93}S_{0.07}, ZrNCl, 1T-TaS₂, and Bi₂Se₃

Yi Cui,^{1,2,*} Ze Hu,^{2,*} Jin-Shan Zhang,^{1,†} Wen-Long Ma,³ Ming-Wei Ma,³ Zhen Ma,⁴
Cong Wang,² Jia-Qiang Yan,⁵ Jian-Ping Sun,⁶ Jin-Guang Cheng,⁶ Shuang Jia,^{3,7,‡}
Yuan Li,^{3,7} Jin-Sheng Wen,^{4,8} He-Chang Lei,² Pu Yu,^{9,7} Wei Ji,² and Wei-Qiang Yu^{2,§}

¹*School of Mathematics and Physics, North China Electric Power University, Beijing, 102206, China*

²*Department of Physics, and Beijing Key Laboratory of Opto-electronic Functional Materials & Micro-nano Devices, Renmin University, Beijing 100872, China*

³*International Center for Quantum Materials, School of Physics, Peking University, Beijing 100871, China*

⁴*National Laboratory of Solid State Microstructures and Department of Physics, Nanjing University, Nanjing 210093, China*

⁵*Materials Science and Technology Division, Oak Ridge National Laboratory, Oak Ridge, Tennessee 37831, USA*

⁶*Beijing National Laboratory for Condensed Matter Physics and Institute of Physics, Chinese Academy of Sciences, Beijing 100190, China*

⁷*Collaborative Innovation Center of Quantum Matter, Beijing 100871, China*

⁸*Innovative Center for Advanced Microstructures, Nanjing University, Nanjing 210093, China*

⁹*State Key Laboratory of Low Dimensional Quantum Physics and Department of Physics, Tsinghua University, Beijing 100084, China*

We report protonation in several compounds by an ionic-liquid-gating method, under optimized gating conditions. This leads to single superconducting phases for several compounds. Non-volatility of protons allows post-gating magnetization and transport measurements. The superconducting transition temperature T_c is enhanced to 43.5 K for FeSe_{0.93}S_{0.07}, and 41 K for FeSe after protonation. Superconducting transitions with $T_c \sim 15$ K for ZrNCl, ~ 7.2 K for 1T-TaS₂, and ~ 3.8 K for Bi₂Se₃ are induced after protonation. Electric transport in protonated FeSe_{0.93}S_{0.07} confirms high-temperature superconductivity. Our ¹H nuclear magnetic resonance (NMR) measurements on protonated FeSe_{1-x}S_x reveal enhanced spin-lattice relaxation rate $1/T_1$ with increasing x , which is consistent with the LDA calculations that H⁺ is located in the interstitial sites close to the anions.

Carrier doping is an effective method for tuning metal-insulator transitions and superconductivity. In addition to chemical substitution, electric gating also emerged as an efficient method for tuning carrier density in thin films. [1–3] With the development of various room-temperature ionic liquids, the transistor-like gating method [4–9] was found to induce a large carrier density for thin films or crystal flakes, through charge polarization. Lithium doping by ionic solid gating was also found to enhance the superconducting transition temperature of thin flakes of FeSe [10]. Recently, tuning of proton or oxygen concentration, using ionic-liquid-gating as a medium, was introduced to modify the lattice structure and magnetism of SrCoO_{2.5} [11]. This H⁺ implantation method was later applied in iron-based superconductors, to induce superconductivity or enhance the superconducting transition temperature in bulk crystals due to an electron doping effect [12].

It is important to note that H⁺ originates from water contamination in the ionic liquid by this method [11]. The advantages of this technique are that H⁺ is non-volatile and the gating is performed near the ambient conditions, which allow various post-gating measurements. However, multiple superconducting phases in pro-

tonated FeSe_{1-x}S_x emerge, indicating that proton concentration is inhomogeneous across the bulk crystals. The magnetization data in the protonated FeSe_{0.93}S_{0.07} show that the volume fraction of the superconducting phase is very low under the reported gating conditions [12].

In this Letter, we report our optimized protonation conditions with this ionic-liquid-gating method, to improve the superconducting volume ratio and the doping homogeneity. The best protonation temperature is found to be 350 K (higher than the room temperature), with a gating period of 12 days. For FeSe_{0.93}S_{0.07}, the superconducting volume ratio is largely enhanced compared to the room temperature gating, as determined by the magnetization measurement. Transport measurement is also succeeded to confirm superconductivity. We also apply the optimized protonation on various layered compounds, including FeSe, insulating ZrNCl, 1T-TaS₂, and Bi₂Se₃, where protonation either induces superconductivity or enhances the T_c largely. In particular for 1T-TaS₂, we achieve a T_c higher than the regular gating method.

In our experiment, pristine FeSe and FeSe_{0.93}S_{0.07} single crystals were made by the vapor transport method [13, 14]. ZrNCl powders were made by the high-pressure synthesis [15]. The 1T-TaS₂ single crystal was grown by the chemical vapor transport method [16]. Bi₂Se₃ was grown by the flux method [17]. FeS single crystal was made by the hydrothermal method [18]. We employ the protonation technique as illustrated in Fig. 1. As shown in Fig. 1, samples are attached to the negative

* These authors contributed equally to this study.

† zhangjs@ncepu.edu.cn

‡ gwljiahuang@pku.edu.cn

§ wqyu.phy@ruc.edu.cn

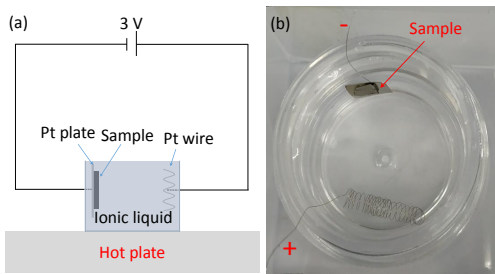


FIG. 1. (a) An illustration of the protonation setup. Platinum electrodes are placed in a container filled with the ionic liquid. The gating voltage is set to be about 3 V. The ionic liquid are heated up to 350 K by a hot plate. (b) A picture of the positive and negative of platinum electrodes, with the sample attached on the negative electrode.

electrodes, and a voltage of 3.0 V is applied as the gating voltage. The ionic liquid EMIM-BF₄ is used. The gating temperature is optimized to be 350 K, which improves proton diffusion efficiency in the crystal. Typical gating period is 12 days when water is nearly fully electrolyzed. The dc magnetization is measured with a magnetic property measurement system (MPMS), and the transport is measured with a physical property measurement system (PPMS). These measurements were successfully performed after gating was removed at the room temperature, which indicates nonvolatile protons are inserted, in contrast to conventional ionic-liquid gating where gating cannot be removed during measurements. The proton NMR is performed by the spin-echo method, and the spin-lattice relaxation rate $1/T_1$ is measured by the inversion recovering method.

In the following, we present protonation measurements on these compounds.

FeSe. Recently, FeSe has attracted a great deal of research attention because of its highly tunable superconductivity. Its T_c is enhanced from 8.5 K to above 40 K under high pressure [19, 20], by chemical intercalation [21–24], by ionic-liquid/solid gating [10, 25], or by dimensional reduction into a single-layer phase [26].

Fig. 2 shows the dc susceptibility $\chi(T)$ of a protonated FeSe single crystal. A rapid drop of χ are clearly at 41 K seen, indicating the onset of superconductivity. Therefore, the T_c of FeSe is also largely enhanced by the protonation technique.

FeSe_{0.93}S_{0.07}. FeSe_{1-x}S_x is a series of compounds, whose T_c ranges between 8 K and 13 K for $x < 0.12$ [27]. Previously, two superconducting transitions, at 25 K and 42.5 K were reported in the protonated sample. Here we show that with increased protonation temperature at 350 K, a single high- T_c phase is realized. Figure 3 shows the dc susceptibility $\chi(T)$ and the resistance data $R(T)$ of a protonated FeSe_{0.93}S_{0.07} single crystal. The susceptibility data shows $T_c \approx 41$ K, seen by the drop of χ (Fig. 3 (a)). By contrast, the resistance data shows a higher onset T_c of 43.5 K as indicted in Fig. 3, by a sudden drop

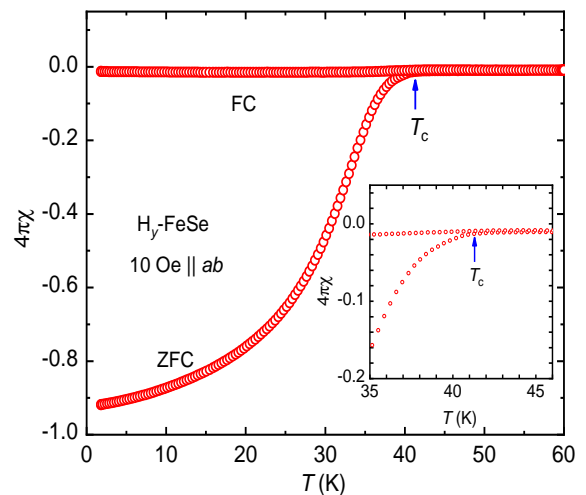


FIG. 2. The dc susceptibility of a protonated FeSe single crystal (size 5mm*5mm*1mm) measured under the field-cooled (FC) and zero-field-cooled (ZFC) conditions with a magnetic field of 10 Oe. The arrows points at the superconducting transition. Inset: An enlarged view of the susceptibility data close to T_c .

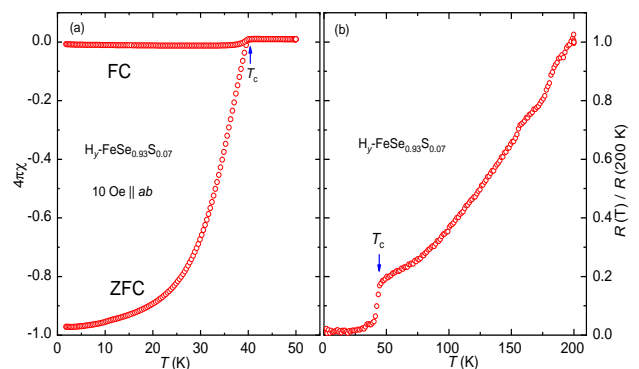


FIG. 3. (a) The dc susceptibility of a H $_{\gamma}$ -FeSe_{0.93}S_{0.07} single crystal as a function of temperature, measured under ZFC and FC conditions. (b) The resistance of the crystal as a function of temperature. The arrows mark the onset temperature of superconductivity.

of resistance upon cooling.

ZrNCl. ZrNCl is a layered material with electric gating or lithium doping. Superconductivity can be induced in ZrNCl by electric gating or lithium doping [3, 4, 28]. We pressed ZrNCl powders into thin pellets and then doped H⁺ with the current ionic-liquid-gating method. The samples turn from blue into black upon proton doping. Figure 4 shows the dc susceptibility of the proton-doped ZrNCl. The sharp drop of χ below 15 K shows the onset of superconductivity, with field up to 1000 Oe. The volume ratio of the superconducting phase, estimated from the ZFC data at 10 Oe field, is about 12%. This suggests that proton doping is very efficient. We note that an ionic-liquid gating on ZrNCl at low temperatures is

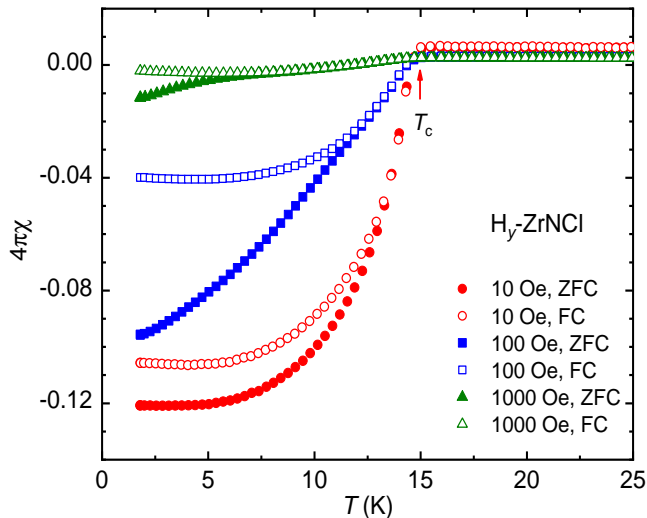


FIG. 4. The dc susceptibility χ of H_y -ZrNCl pellets, measured under FC and ZFC condition with different fields. The arrow marks the onset temperature of superconductivity.

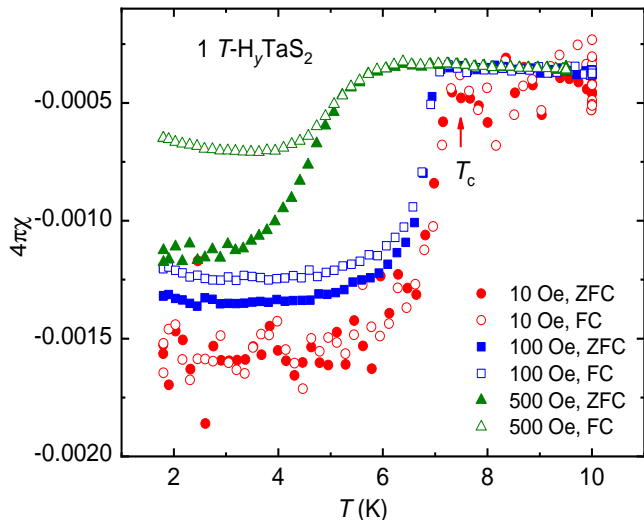


FIG. 5. The dc susceptibility χ of a protonated $1T$ -TaS₂ single crystal, measured under FC and ZFC condition, under various fields. The arrow marks the onset of the superconducting transition.

also reported, which proposes that the depletion of Cl⁻ concentration causes superconductivity [29].

1T-TaS₂. $1T$ -TaS₂ is a layered compound with a triangular lattice. It goes through a series of charge-density-wave (CDW) transitions upon cooling [30, 31]. Superconductivity can be achieved by chemical doping, where the highest T_c is achieved at 3.5 K [32]. Here we performed protonation on $1T$ -TaS₂ single crystals. The dc magnetization of a protonated sample is shown in Fig. 5, measured under FC and ZFC conditions at different fields. The superconducting transition temperature T_c is found to be ~ 7.2 K under 10 Oe field. We note that this tran-

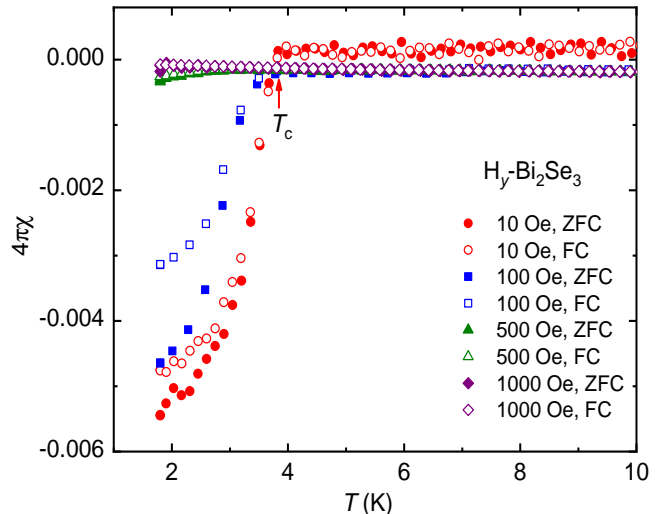


FIG. 6. The dc susceptibility χ of a protonated Bi₂Se₃ single crystal, measured under FC and ZFC condition at different fields. The arrow marks the onset of superconducting transition at T_c .

sition temperature is higher than that achieved by the chemical doping. With an applied field of 500 Oe, the superconducting transition is still observed.

Bi₂Se₃. As a topological insulator, Bi₂Se₃ has caused a lot of research interests [33, 34]. Superconductivity can be achieved upon Cu or Sr doping into this material [35, 36]. Here we find that by protonation, superconductivity can also be achieved. As seen in Fig. 6, the superconducting transition temperature T_c is found to be 3.8 K, which is close to that reported by the chemical doping. With an applied field of 500 Oe, superconductivity is highly suppressed. Since protonation does not induce chemical substitution, our study indicates that chemical doping in the interstitial sites is important for the occurrence of superconductivity. Further studies on the protonation of induced superconductivity in this compound, regarding to possible topological superconductivity, are demanded.

¹H NMR studies on H_y FeSe_{1-x}S_x: In H_y FeSe_{1-x}S_x compounds, intrinsic ¹H NMR spectra was observed. Figure 7 shows the ¹H spin-lattice relaxation rates divided by temperatures, versus temperature for protonated FeSe_{1-x}S_x with $x=0, 0.07$ and 1. Above 50 K, $1/T_1T$ stays nearly constant but varies with x , which indicate that doped protons are detected by the current measurements. Indeed, the increase of $1/T_1$ with increasing x is consistent with the LDA calculations that H⁺ is inserted in the interstitial sites as discussed below. Since the c -axis lattice parameter is reduced with increasing x [27], the hyperfine coupling between ¹H and the FeSe plane increases with increasing S²⁻ concentration.

Our LDA calculations indicate that H⁺ is located in the interstitial sites close to the anion Se²⁻/S²⁻, as

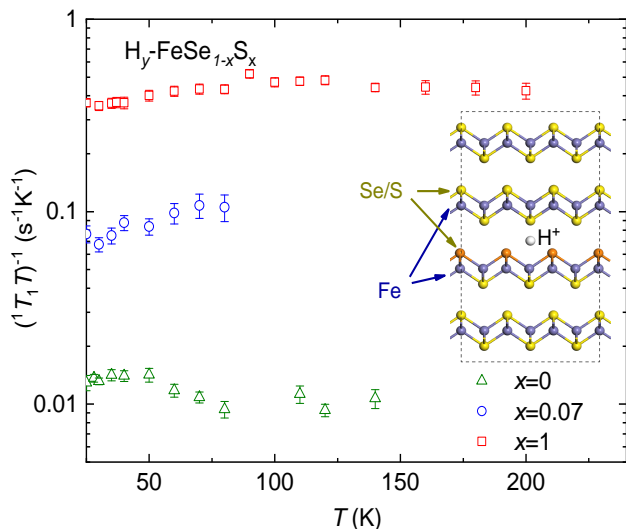


FIG. 7. The ^1H spin-lattice relaxation rate divided by temperature $1/T_1T$ of $\text{H}_y\text{FeSe}_{1-x}\text{S}_x$ single crystals, measured with a magnetic field of 5 T along the c -axis. Inset: The proton position in the lattice obtained by the LDA calculations.

TABLE I. T_c of the materials before and after protonation

Compound	FeSe	$\text{FeSe}_{0.93}\text{S}_{0.07}$	ZrNCl	1T-TaS ₂	Bi_2Se_3
T_c before protonation	9 K	8 K	0	0	0
T_c after protonation	41 K	43.5 K	15 K	7.2 K	3.8 K

shown by the schematic drawing in the inset of Fig. 7. This can be understood as an effect of coulomb attraction between H^+ and $\text{Se}^{2-}/\text{S}^{2-}$. So far, we have found that this doping method is efficient in layered compounds,

which indicates that H^+ is most likely doped between the layers as in $\text{H}_y\text{FeSe}_{1-x}\text{S}_x$.

Discussions and summary. Our XRD measurement did not resolve the change of lattice structure after protonation, which suggests that the chemical pressure effect of proton insertion is possibly very small. As a result, an electron-doping should be primarily responsible for the change of T_c .

In Table 1, we summarize all the T_c of different compounds, before and after protonation under the current optimized conditions. The optimization at 350 K suggests that the efficiency of proton doping is caused by a balance between proton diffusion into the sample and the evasion out of the sample, both of which increase with temperature. The current method supplies a universal electron doping method, which could be widely used in tuning and searching for superconductivity and metal-insulator transitions in the layered compounds.

Work at RUC was supported by the National Natural Science Foundation of China with Grand Nos. 51872328, 11622437, 11574394, 11774423, and 11822412, the Strategic Priority Research Program of Chinese Academy of Sciences (Grant No. XDB30000000), the Ministry of Science and Technology of China with Grand No. 2016YFA0300504, the Fundamental Research Funds for the Central Universities, and the Research Funds of Renmin University of China (RUC) (15XNLQ07, 18XNLG14, 19XNLG17). SJ was supported by the National Natural Science Foundation of China with Grand Nos. 11774007 and U1832214. YC was supported by the Outstanding Innovative Talents Cultivation Funded Programs 2018 of Renmin University of China. JQY was supported by the U.S. Department of Energy, Office of Science, Basic Energy Sciences, Division of Materials Sciences and Engineering.

- [1] Ahn C H, Bhattacharya A, Ventra M D, Eckstein J N, Frisbie C D, Gershenson M E, Goldman A M, Inoue I H, Mannhart J, Millis A J, Morpurgo A F, Natelson D and Triscone J-M 2006 Rev. Mod. Phys. **78** 1185
- [2] Ueno K, Nakamura S, Shimotani H, Ohtomo A, Kimura N, Nojima T, Aoki H, Iwasa Y and Kawasaki M 2008 Nature Mater. **7** 855
- [3] Saito Y, Kasahara Y, Ye J, Iwasa Y and Nojima T 2015 Science **350** 409
- [4] Ye J T, Inoue S, Kobayashi K, Kasahara Y, Yuan H T, Shimotani H and Iwasa Y 2010 Nature Mater. **9** 125
- [5] Bollinger A T, Dubuis G, Yoon J, Pavuna D, Misewich J and Bozović I 2011 Nature **472** 458
- [6] Ye J T, Zhang Y J, Akashi R, Bahramy M S, Arita R and Iwasa Y 2012 Science **338** 1193
- [7] Li L J, O'Farrell E C T, Loh K P, Eda G, Özyilmaz B and Castroneto A H 2015 Nature **529** 185
- [8] Lu J M, Zheliuk O, Leermakers I, Yuan N F Q, Zeitler U, Law K T and Ye J T 2015 Science **350** 1353
- [9] Miyakawa T, Shiogai J, Shimizu S, Matsumoto M, Ito Y, Harada T, Fujiwara K, Nojima T, Itoh Y, Aida T, Iwasa Y and Tsukazaki A 2018 Phys. Rev. Materials **2** 031801
- [10] Lei B, Wang N Z, Shang C, Meng F B, Ma L K, Luo X G, Wu T, Sun Z, Wang Y, Jiang Z, Mao B H, Liu Z, Yu Y J, Zhang Y B and Chen X H 2017 Phys. Rev. B **95** 020503
- [11] Lu N, Zhang P, Zhang Q, Qiao R, He Q, Li H-B, Wang Y, Guo J, Zhang D, Duan Z, Li Z, Wang M, Yang S, Yan M, Arenholz E, Zhou S, Yang W, Gu L, Nan C-W, Wu J, Tokura Y and Yu P 2017 Nature **546** 124
- [12] Cui Y, Zhang G, Li H, Lin H, Zhu X, Wen H-H, Wang G, Sun J, Ma M, Li Y, Gong D, Xie T, Gu Y, Li S, Luo H, Yu P and Yu W 2018 Sci. Bull. **63** 11
- [13] Böhmer A E, Hardy F, Eilers F, Ernst D, Adelman P, Schweiss P, Wolf T and Meingast C 2013 Phys. Rev. B **87** 180505
- [14] Hosoi S, Matsuura K, Ishida K, Wang H, Mizukami Y, Watashige T, Kasahara S, Matsuda Y and Shibauchi T 2016 Proc. Natl. Acad. Sci. USA **113** 8139
- [15] Chen X, Koiwasaki T and Yamanaka S 2002 J. Phys.

- Condens. Matter **14** 11209
- [16] Kuwabara M, Tomita M, Hashimoto H and Endoh H 1986 Phys. Stat. Sol. **96** 39
- [17] Sultana R, Awana G, Pal B, Maheshwari P K, Mishra M, Gupta G, Gupta A, Thirupathaiah S and Awana V P S 2017 J. Supercond. Nov. Magn. **30** 2031
- [18] Borg C K H, Zhou X, Eckberg C, Campbell D J, Saha S R, Paglione J and Rodriguez E E 2016 Phys. Rev. B **93** 094522
- [19] Medvedev S, McQueen T M, Troyan I A, Palasyuk T, Erements M I, Cava R J, Naghavi S, Casper F, Ksenofontov V, Wortmann G and Felser C 2009 Nature Mater. **8** 630
- [20] Sun J P, Matsuura K, Ye G Z, Mizukami Y, Shimozawa M, Matsubayashi K, Yamashita M, Watashige T, Kasahara S, Matsuda Y, Yan J-Q, Sales B C, Uwatoko Y, Cheng J-G and Shibauchi T 2016 Nature Commun. **7** 12146
- [21] Guo J, Jin S, Wang G, Wang S, Zhu K, Zhou T, He M and Chen X 2010 Phys. Rev. B **82** 180520
- [22] Hatakeda T, Noji T, Kawamata T, Kato M, and Koike Y 2013 J. Phys. Soc. Jpn. **82** 123705
- [23] Dong X, Zhou H, Yang H, Yuan J, Jin K, Zhou F, Yuan D, Wei L, Li J, Wang X, Zhang G and Zhao Z 2015 J. Am. Chem. Soc. **137** 66
- [24] Lu X F, Wang N Z, Wu H, Wu Y P, Zhao D, Zeng X Z, Luo X G, Wu T, Bao W, Zhang G H, Huang F Q, Huang Q Z and Chen X H 2015 Nature Mater. **14** 325
- [25] Lei B, Cui J H, Xiang Z J, Shang C, Wang N Z, Ye G J, Luo X G, Wu T, Sun Z and Chen X H 2016 Phys. Rev. Lett. **116** 077002
- [26] Wang Q-Y, Li Z, Zhang W-H, Zhang Z-C, Zhang J-S, Li W, Ding H, Ou Y-B, Deng P, Chang K, Wen J, Song C-L, He K, Jia J-F, Ji S-H, Wang Y-Y, Wang L-L, Chen X, Ma X-C and Xue Q-K 2012 Chin. Phys. Lett. **29** 037402
- [27] Mizuguchi Y, Tomioka F, Tsuda S, Yamaguchi T and Takano Y 2009 J. Phys. Soc. Jpn. **78** 074712
- [28] Taguchi Y, Kitora A and Iwasa Y 2006 Phys. Rev. Lett. **97** 107001
- [29] Zhang S, Gao M-R, Fu H-Y, Wang X-M, Ren Z-A and Chen G-F 2018 Chin. Phys. Lett. **35** 097401
- [30] Wilson J A, Di Salvo F J and Mahajan S 1975 Adv. Phys. **24** 117
- [31] Thomson R E, Burk B, Zettl A and Clarke J 1994 Phys. Rev. B **49** 16899
- [32] Liu Y, Ang R, Lu W J, Song W H, Li L J and Sun Y P 2013 Appl. Phys. Lett. **102** 192602
- [33] Zhang H, Liu C X, Qi X L, Dai X, Fang Z and Zhang S C 2009 Nature Phys. **5** 438
- [34] Xia Y, Qian D, Hsieh D, Wray L, Pal A, Lin H, Bansil A, Grauer D, Hor Y S, Cava R J and Hasan M Z 2009 Nature Phys. **5** 398
- [35] Hor Y S, Williams A J, Checkelsky J G, Roushan P, Seo J, Xu Q, Zandbergen H W, Yazdani A, Ong N P and Cava R J 2010 Phys. Rev. Lett. **104** 057001
- [36] Liu Z, Yao X, Shao J, Zuo M, Pi L, Tan S, Zhang C and Zhang Y 2015 J. Am. Chem. Soc. **137** 10512